Genomic surveillance revealed the prevalence of unique SARS-CoV-2 variant bearing mutation in the RdRp gene among Nevada patients

Paul D. Hartley[1,5*], Richard L. Tillett[8*], Yanji Xu[6], David P. AuCoin[3,4], Joel R. Sevinsky[7], Andrew Gorzalski[2], Mark Pandori[2,4], Cyprian C. Rossetto[3,4*#], Subhash C. Verma[3,4*#]

[1] Nevada Genomics Center, Research & Innovation
[2] Nevada State Public Health Lab
[3] Department of Microbiology & Immunology
[4] School of Medicine, University of Nevada, Reno
[5] University of Nevada, Reno
[6]Nevada Center for Bioinformatics, Research & Innovation
[7]Theiagen Consulting LLC
[8] Nevada Institute of Personalized Medicine, University of Nevada, Las Vegas,
* These authors contributed equally to this work and are listed in alphabetical order

[#] To whom correspondence should be addressed:
Cyprian C. Rossetto crossetto@med.unr.edu, Subhash C. Verma
scverma@med.unr.edu

Running title: Unique RdRp variant of SARS-CoV-2 in Nevada patients

Keywords: SARS-CoV-2, COVID-19, genome enrichment, nsp12, RdRp, orf1b 314

ABSTRACT:

Background:

SARS-CoV-2 is the etiological agent of coronavirus disease 2019 (COVID-19), which has a wide range of disease manifestations, including relatively mild respiratory illness to severe disease requiring hospitalization. Patients with signs of COVID-19 (fever, coughing, shortness of breath) were tested for the virus by targeting specific SARS-COV-2 genomic loci via RT-PCR using RNA extracted from nasopharyngeal/nasal swabs. However, this testing does not yield genetic information required for identifying viral evolution or variants.

Methods:

We sequenced 200 specimens from positively identified cases in Nevada through our robust protocol for sequencing SARS-CoV-2 genomes directly from patients nasopharyngeal/nasal swabs. This protocol enabled identification of specific nucleotide variants including those for D614G and clade defining mutations. Additionally, these sequences were used to determine the phylogenetic relationships of SARS-CoV-2 genomes of public health importance occurring in the state of Nevada.

Results:

Our study reports the finding of a novel variant in the nsp12 (RdRp-RNA dependent RNA Polymerase) protein at residue 323 (314aa of orf1b) to Phenylalanine (F) from Proline (P), present in the original isolate of SARS-CoV-2 (Wuhan-1). This 323F variant is found at a very high frequency in Northern Nevada suggesting for a founder effect. Structural modeling of the RdRP with P323F mutation did not show any significant difference in

protein conformation but the phenotypic effect is unknown and an area of active investigation.

Conclusions:

Our results highlight the introduction and spread of specific SARS-CoV-2 variants at very high frequency within a distinct geographic location that is important for clinical and public health perspectives in understanding the evolution and transmission of SARS-CoV-2.

BACKGROUND:

Severe Acute Respiratory Syndrome coronavirus 2 (SARS-CoV-2), the cause of coronavirus disease 2019 (COVID-19), was first identified and reported in December 2019 in Wuhan, Hubei province, China [1-3]. RNA sequencing and phylogenetic analysis of a specimens taken during the initial outbreak in Wuhan determined that the virus is most closely related (89.1% nucleotide similarity) to a group of SARS-like coronaviruses (genus Betacoribavirus, subgenus Sarbecovirus) which had previously been identify in bats in China [2, 4]. Coronaviruses have a recent history as emerging infections, first SARS-CoV in 2002-2003, and Middle East respiratory syndrome coronavirus (MERS-CoV) in 2012, both zoonotic infections that cause severe respiratory illness in humans [2, 5-8] [2,5-8]. Unlike SARS-CoV and MERS-CoV which displayed limited global spread, SARS-CoV-2 has spread around the world within a few months. There are specific characteristics of SARS-CoV-2 which have facilitated the transmission, including infections that result in asymptomatic or mild disease, allowing for under-characterized transmission.

71 SARS-CoV-2 is an enveloped, positive single-stranded RNA virus. Detection of
72 SARS-CoV-2 in patients has primarily occurred using RT-qPCR to detect viral RNA from
73 respiratory specimens (primarily nasal, nasopharyngeal swabs). While RT-PCR results
74 can be quantified through determination of a cycle threshold (Ct) value for each sample
75 it does not yield sequence data leading to the description of genomic variants. To further
76 a study of such variants, and to better understand the epidemiology of the virus in the
77 state of Nevada, we developed a workflow that allowed us to sequence SARS-CoV-2
78 genomic RNA from patient swabs containing a broad range of viral loads. Of the
79 sequences of SARS-CoV-2 currently submitted to common database, several were
80 obtained after the virus had been passed in Vero cells [9, 10] and others came directly
81 from patient specimens [11, 12]. Certain data has suggested a potential for lab acquired
82 mutations following passage in cell culture [9, 13]. Specifically, a report of SARS-CoV-2
83 passage in Vero cells which resulted in a spontaneous 9 amino acid deletion within the
84 spike (S) protein that overlaps with furin cleavage site [13]. The loss of this site is
85 suggested to increase the viral entry into Vero cells [14]. For both research and
86 epidemiological purposes, sequencing of SARS-CoV-2 directly from patient specimens
87 not only reduces the possibility of lab-adapted mutations following passage in cell culture
88 but also reduces the time that would be spent growing the virus from the patient
89 specimens and subsequently also reduces handling larger amounts of infectious virus.
90 Additionally, one of the goals in developing an optimized SARS-CoV-2 NGS protocol was
91 to be able to generate adequate depth of coverage of the viral genome while minimizing
92 the sequencing of non-viral RNA which would allow for more specimens to be multiplexed
93 together during sequencing.

94 Our workflow employs a combination of RNA amplification, conversion into
95 Illumina-compatible sequencing libraries and enrichment of SARS-CoV-2 library
96 molecules prior to sequencing. Using this novel methodology, we sequenced SARS-
97 CoV-2 from a total of 200 patient specimens collected over a 3-month period originating
98 from Nevada. Of the 200 selected, 173 were sequenced with enough quality to be used
99 for determining SARS-CoV-2 nucleotide variants to perform further phylogenetic analysis
100 and study the viral epidemiology within the state of Nevada. Analysis of the data suggests
101 a specific epidemiological course for the local epidemic within Northern Nevada. This was
102 characterized by an initial observation of variants closely resembling isolates originating
103 directly from China or Europe. Subsequent to government-mandated period of restrictions
104 on business and social activity, we observed that a viral isolate not seen elsewhere in the
105 world emerged within Northern Nevada cases (nucleotide 14,407 and 14,408). This
106 isolate contains an amino acid change in residue P323L/F of the RdRp (nsp12).
107 Furthermore, we found that sampled viral isolates in Southern Nevada, unlike those in
108 Northern Nevada, closely resembled the makeup of the United States in general.
109
110 **METHODS:**
111 **SARS-CoV-2 specimen and library preparation.** Nasal and Nasopharyngeal swab
112 specimens were received at the Nevada State Public Health Lab (NSPHL) or Southern
113 Nevada Public Health Lab (SNPHL) and RNA extraction was completed using either a
114 QIAamp Viral RNA Mini Kit (QIAGEN) or Mag-Bind Viral DNA/RNA kit (Omega Biotek).
115 Specimens were tested for the presence of coronaviral RNA using FDA-approved kits
116 that employed RT-PCR to detect SARS-COV-2 RNA.

117 A set of 200 coronavirus positive specimens were selected for genome
118 sequencing. Specimens were treated with DNase I (QIAGEN) for 30 minutes at room
119 temperature and concentrated using RNeasy Minelute spin columns (QIAGEN) based on
120 the manufacturer supplied protocol. These concentrated samples were converted into
121 Illumina-compatible sequencing libraries with a QIAseq FX Single Cell RNA Library kit
122 (QIAGEN). RNA samples were annealed to a 1:12.5 dilution of QIAseq FastSelect -HMR
123 probes (QIAGEN) to reduce subsequent amplification of human ribosomal RNA. After
124 treatment to remove trace DNA from the samples, a reverse transcription reaction was
125 carried out using random hexamers. The synthesized DNA was ligated to one another,
126 followed by isothermal linear amplification. Amplified DNA (1 μg) was enzymatically
127 sheared to an average insert size of 300 bp, and Illumina-compatible dual-indexed
128 sequencing adapters were ligated to the ends. Next, about 300 ng of adapter-ligated
129 sample was amplified with 6 cycles of PCR with KAPA HiFi HotStart polymerase (Roche
130 Sequencing Solutions). Enrichment of library molecules containing SARS-CoV-2
131 sequence was conducted with a myBaits kit and coronavirus-specific biotinylated probes
132 (Arbor Biosciences). Each enrichment used 500 ng of PCR-amplified DNA, was carried
133 out based on manufacturer instructions at a hybridization temperature of 65° for 16 hours,
134 and was completed with 8-16 cycles of PCR using KAPA HiFi HotStart polymerase.
135 Samples were sequenced using an Illumina Next-seq mid-output (2 x 75). The generated
136 FASTQ files from the sequencing reaction were analyzed as described below. The data
137 files are available at GISAID, NCBI under the
138 https://www.ncbi.nlm.nih.gov/bioproject/657893

139 **Computational analysis.** Sequence pair libraries were trimmed using Trimmomatic,
140 version 0.39 and adapter-clipping setting “2:30:10:2:keepBothReads” [15]. Read pairs
141 were aligned against the Wuhan reference genome (NC_045512.2) by Bowtie 2, version
142 2.3.5, local alignment [16]. PCR optical duplicates were removed via Picard
143 MarkDuplicates [17].

144 Variants were called using Freebayes, version 1.0.2, with ploidy set to 1, minimum
145 allele frequency 0.75, and minimum depth of 4 [18]. No variants were called in the first
146 200 bp and final 63 bp of the COVID-19 genome. High-quality variant sites were selected
147 where site “QUAL > 20” using *vcffilter*, VCFlib version 1.0.0_rc2 [19]. Individual genomes
148 were reconstructed by their filter-passing variants using *bcftools consensus* and only
149 where aligned coverage depth ≥ 4; bases with coverage below four are reported as
150 unknown (Ns) [20].

151 A set of 3,644 complete, high-coverage SARS-CoV-2 genomes reported in the
152 July 15, 2020 Nextstrain.org global subsample and metadata were obtained from GISAID
153 and combined with our own samples to determine their phylogenetic placement [21, 22].
154 Four of the global samples were set aside after screening for unexpected FASTA
155 characters. The combined sets of global and Nevadan samples were aligned together,
156 with metadata, by the *augur* phylodynamic pipelines of the *ncov* build of the *nextstrain*
157 command-line tool, version 2.0.0.post1 [23].

158 Cumulative frequency of D614G, clades (19A, 19B, 20A, 20B, 20C), and P323L/F
159 were calculated at each time point based on the total number of specimens up to the
160 indicated date. Plots and pie charts were generated using GraphPad Prism (version 8).

161 **nsp12 protein modeling.** Sequence of nsp12 (RdRp) protein for SARS-CoV-2
162 (YP_009725307.0) was retrieved from NCBI protein database and 3D model was
163 structured based on a previously published report (PDB ID: 6XEZ [24]. In addition to
164 nsp12 (chain A), the model also contains nsp7 (chain C), nsp8 (chain B and D), nsp13
165 (chain E and F), ligands (ZN, Mg) and RNA template and product strands. Mutational
166 changes to residue 323 within nsp12 were performed using PyMol Molecular Graphics
167 System (version 2.0, Schrödinger LLC). The original proline (P) was mutated to either
168 leucine (L) or phenylalanine (F) as indicated, these residues along with residues
169 containing side chains within 5 Å of P323L/F are shown as sticks. The rotamers for each
170 P323L/F were assessed and those with least rotational strain and steric hindrance were
171 used to generate the final image. To determine any NCBI deposited sequences which
172 contain the P323F variant, standard protein BLAST from the BLASTp suite was used to
173 find nsp12 protein sequences which contained FSTVFP**F**TSFGP (P323F is bold and
174 underline) from full length SARS-CoV-2 genomes. The P323F amino acid changes were
175 confirmed with the NCBI deposited nucleotide sequences.
176
177 **RESULTS:**
178 **RNA-seq workflow and assembly of SARS-CoV-2 genomes.**
179 A total of 200 SARS-CoV-2 positive specimens collected in Nevada from March
180 6th to June 5th were randomly selected to have their viral genomes sequenced for variant
181 analysis and subsequent epidemiological studies (Fig 1A and Materials & Methods). Of
182 the sequenced specimens, 173 had >90% coverage and sufficient depth to accurately
183 call those genomic positions with variants (Fig. 1B). An alignment of SARS-CoV-2

184 genomes from these specimens is presented as supplemental data (Supplemental Fig.
185 S1) showing 173 specimens with over 90% coverage. These 173 specimens represented
186 133 patient specimens from Northern Nevada (including Washoe County of which Reno
187 is the major city, the Carson-Tahoe area, and other northern, rural counties), 40 patient
188 specimens from Southern Nevada (Clark county which encompasses Las Vegas).
189 Nucleotide similarity and variants were determined and used to measure the phylogenetic
190 relationships (Supplemental Fig. S2). The combined nucleotide diversity across the entire
191 SARS-CoV-2 genome for the Nevada specimens is shown in figure 1D, along with the
192 genomic areas that were assessed for change in frequency corresponding to amino acids
193 D614G, P323L/F and nucleotide 379.

194 During the sequencing analysis we also examined the correlation between Ct
195 values from the diagnostic RT-PCR and percentage coverage of the viral genome to
196 determine the performance and robustness of our sequencing method in relation to
197 available viral RNA in a specimen of a given Ct (Fig. 1C). In general, a Ct value less than
198 31 resulted in at least 90% coverage to the SARS-CoV-2 genome. Importantly, our in-
199 house developed method for viral genome enrichment and sequencing directly from the
200 patient's specimens (nasal and nasopharyngeal swabs) was robust and yielded
201 sequences covering over 90% of the genome even in samples having very high Ct (~40)
202 of viral genome detection. This is highly significant and shows the power of our workflow
203 in sequencing of SARS-CoV-2 genome from a spectrum of samples including the ones
204 having inadequate amounts of specimen (due to the variability in collection) or lower viral
205 loads in nasal secretions. Consequently, our sequencing protocol avoids any molecular
206 epidemiological bias, which may get acquired through cell culture-based amplification

207 especially in those specimens with high Ct (low viral load) as our method eliminates the
208 need of virus culture.

209 **Prevalence of amino acid variant D614G of SARS-CoV-2 spike protein in specimens**
210 **collected in Nevada.** Earlier studies have revealed the emergence, spread and potential
211 importance of an alteration, D614G (genomic change at 23403A>G), of the spike protein
212 [25]. This missense mutation has become a clade-distinguishing locus that differentiates
213 viral isolates originating in Asia from those that have emerged from Europe. A total of 173
214 cases were analyzed to determine the number and relative proportion of the specimens
215 which carried the D614G spike protein variant in Nevada. The cumulative frequency for
216 D614 and G614 were plotted from March 6th to June 5th (Fig. 2A). Specimens from the
217 beginning of March represent the earliest known cases in Nevada, and of the 14
218 specimens sequenced during this time period (March 6-March 15) D614 was the
219 predominant variant. This shifted from March to June with an increasing frequency of the
220 G614 allele. The trend for specimens originating from either Northern Nevada (N-NV) and
221 Southern Nevada (S-NV) both show a higher frequency of G614 (Fig. 2B). We used a
222 subsampling of sequence data from Nextstrain.org to assess the frequency of D614G in
223 the United States and globally during the same time period (March 6th to June 5th) (Fig.
224 2B and 2C). The global trend by continent of D614G is also similar, with G614 at a higher
225 frequency, the one noted exception is in Asia, where D614 and G614 continue to exist in
226 equal proportions (Fig. 2C).

227 **Frequency of SARS-CoV-2 clades in Nevada.** Worldwide, there are currently 5 main
228 clades (19A, 19B, 20A, 20B, 20C) of SARS-CoV-2 differentiated based on specific
229 nucleotide profiles in the Year-letter scheme of https://clades.nextstrain.org. Clade 19A

230 and 19B are defined by C8782T and T28144C respectively. 20A is a derivative of 19A
231 and contains mutations C3037T, C14408T and A23403G (resulting in D614G). 20B is
232 defined by mutations G28881A, G28882A and G28883C, and 20C contains C1059T and
233 G25563T [26].

234 To assess the introduction and spread of the clades in Nevada the cumulative
235 frequency for the clades were plotted from March 6th to June 5th (Fig. 3A). The earliest
236 sequenced specimens from Nevada were collected in the beginning of March (March 6-
237 March 15) and are predominantly from clades 19A and 19B. Additional sequenced
238 specimens collected from March to June revealed a shift to a higher frequency of 20C
239 (Fig. 3A). We performed phylogenetic reconstruction of the Nevada specimens and
240 differentiated the clades on the circular dendrogram by color (Fig. 3B). There were
241 discordant trends in the dominant clade for specimens originating from either Northern
242 Nevada (N-NV) and Southern Nevada (S-NV) (Fig. 3C and 3D). Specimens from
243 Northern Nevada (Washoe County, Carson-Tahoe, and other counties) showed a
244 prevalence of 20C, while the Southern Nevada specimens from Clark county had a larger
245 proportion of 20A (Fig. 3C and Supplemental Fig. S3a). We used a subsampling of
246 Nextstrain.org data to assess the frequency of clades in the United States and globally
247 by continent during the same time period (March 6th to June 5th). The dominant clade in
248 the United States was 20C, similar to the frequency seen in the total Nevada samples (N-
249 NV and S-NV) (Fig. 3A and 3C). The global clade distributions were variable in areas
250 outside of Asia while clades 19A and 19B are noted to be more prevalent in Asia. (Fig.
251 3D).

252 **Prevalence of amino acid variant P323L/F of SARS-CoV-2 nsp12 (RdRp) in Nevada.**
253 Analysis of sequencing data revealed a novel observation for our specimens at bases
254 14,407 and 14,408 which results in a change at residue 323 in nsp12 (RdRp). For the
255 Wuhan isolate at 14,407 and 14,408 there is CC for proline (P), the variants have CT for
256 leucine (P323L) and TT for phenylalanine (P323F). To assess the introduction and spread
257 of P323L/F in Nevada, the cumulative frequency of P323, L323 and F323 were plotted
258 from March 6th to June 5th (Fig. 3A). Nevada specimens from the beginning of March
259 (March 6-March 15) show P323 was the predominant variant. As additional specimens
260 were collected and sequenced from March to June there was a shift to a higher frequency
261 of L323 and F323 (Fig. 4A). We performed phylogenetic reconstruction of the Nevada
262 specimens and noted the P323L/F variants on the circular dendrogram with the indicated
263 colors (Fig. 4B). Interestingly, analysis of the Northern Nevada and Southern Nevada
264 specimen showed very different dominant variants (Fig. 4B). In Northern Nevada the
265 F323 was more prevalent, and in Southern Nevada L323 was more prevalent. We used
266 a subsampling of Nextstrain.org data to assess the frequency of P323L/F in the United
267 States and globally during the same time period (March 6th to June 5th). P323 is the
268 predominant variant in Asia, while L323 is more prevalent in other areas of the world and
269 F323 is only appreciably noted in North America (Fig. 4D and 4E).
270
271 **DISCUSSION:**
272 We have developed a novel method which combines specific depletion and
273 enrichment strategies that results in efficient SARS-CoV-2 RNA-seq with high genome
274 coverage and depth. An advantage of this protocol is that it generates sequence data

275 directly from swab specimens without the need to passage the virus in cell culture thereby
276 reducing the handling of infectious material and induction of culture-acquired mutations.
277 Another obstacle in sequencing directly from swab specimens is that most FDA-approved
278 commercially available RNA extraction kits are specifically optimized to recover low
279 amounts of total nucleic acids, include carrier polyA RNA that could be convertible into
280 sequence able molecules, as has been observed previously with RNA-seq of Lassa- or
281 Ebola-positive clinical specimens [27].

282 The workflow incorporates amplification of low-abundance RNA into micrograms
283 of DNA, followed by conversion from a fraction of the DNA into Illumina-compatible
284 sequencing libraries and enrichment of these libraries for SARS-CoV-2 sequences. In
285 addition, during the reverse transcription step a reagent was incorporated to reduce the
286 subsequent amplification of host ribosomal RNA. This approach is robust in that it
287 converts low amounts of RNA into microgram quantities of DNA representative of all the
288 RNA species (aside of rRNA) present in the specimen. This DNA can be stored
289 indefinitely to be interrogated by multiple techniques at a later date. Additionally, RNA
290 amplification is likely less sensitive to low viral abundance compared to RT-PCR. Finally,
291 the use of probes to enrich for coronavirus-specific sequencing library molecules is less
292 sensitive to variants compared to tiling PCR amplicon approaches [28-32].

293 The data herein implicate that early in the pandemic, before the “stay-at-home”
294 order on April 1st, there were multiple introductions of SARS-CoV-2 into the state of
295 Nevada. From April 1st to the beginning of June Nevada experienced a period of semi-
296 isolation, as the casinos and most hotels shut down, tourism and travel to the state
297 essentially stopped. Because of the stay-at-home order and social distancing measures

298 put in place there was less mobility of people within and between states. It is possible that
299 these measures, compounded by potential inherent transmission variability of some viral
300 isolates, influenced the change in the frequency of D614G, clades and P323L/F that we
301 noted during this time period within Nevada. In addition, we also found 379C>A had a
302 high prevalence in our study specimens compared to the subsampling of sequences from
303 the United States and international (supplemental Fig. S4). This is a synonymous
304 mutation in nsp1, hence the biological relevance of this nucleotide variant remains to be
305 elucidated.

306 Of the 14,885 complete SARS-CoV-2 genomes currently available (as of August
307 14, 2020) in NCBI there are only 6 genomes that have the P323F variant (accession
308 number: MT706208, LR860619, MT345877, MT627429, MT810889, MT811171). In this
309 study 62 of the 133 specimens from Northern Nevada contain P323F. That is 46% of
310 specimens from Northern Nevada contain P323F compared to 0.04% of NCBI deposited
311 SARS-CoV-2 isolates. We performed structural modeling of the P323L/F variation and
312 did not find any significant change to the nsp12 confirmation with either P323L or P323F
313 (Supplemental Fig. S5), therefore this variant is most likely a neutral mutation and does
314 not confer either a fitness advantage or disadvantage to transmission or pathogenicity of
315 SARS-CoV-2.

316 We find that the overall trend for D614G in Nevada during this time period was
317 similar to what was observed in other states and internationally, with the exception of
318 within Asia where the D614 allele had originated. We noted that there were differences
319 between Northern Nevada and Southern Nevada. In Northern Nevada clade 20C and
320 F323 were more frequent, while during this same time period in Southern Nevada clade

321 20A and L323 were more prevalent. These data indicate that there were distinct genomic
322 profiles of the SARS-CoV-2 viruses that were circulating in these populations during the
323 initial months of the pandemic while stay-at-home order were in place to help prevent
324 transmission of the virus.
325
326 **CONCLUSIONS:**
327 SARS-COV-2 is currently a global pandemic on a scale that has not been experienced
328 since the 1918 influenza pandemic. Viral genomes accumulate nucleotide variations while
329 passing in the human population and these mutations may confer phenotypic differences
330 including immune response and anti-viral drug resistance. We have developed a protocol
331 to enrich SARS-CoV-2 RNA directly from patient nasal/nasopharyngeal specimens that
332 does not rely on amplicon based sequencing strategies nor the need of passing the virus
333 into tissue culture and reducing the possible introduction of lab-adapted mutations. These
334 specimens were subjected to next generation sequencing (NGS) to determine the
335 phylogenetic relationship of SARS-CoV-2 sequences within Nevada during the early
336 months (March to June) of the pandemic. Our study identified a very rare mutation in the
337 RdRp protein (P323F) found to occur at a very high frequency among patients of Nevada.
338 This may be important for clinical and public health perspectives in understanding the
339 transmission and evolution of SARS-CoV-2 as it circulates in humans.
340
341 **DATA AVAILABILITY:**
342 All sequences are available at bio project:
343 https://www.ncbi.nlm.nih.gov/bioproject/657893. All reported data are deposited and

available at GISAID with the following accession numbers: EPI_ISL_515409, EPI_ISL_515407, EPI_ISL_515408, EPI_ISL_515375, EPI_ISL_515376, EPI_ISL_515373, EPI_ISL_515374, EPI_ISL_515371, EPI_ISL_515372, EPI_ISL_515370, EPI_ISL_515416, EPI_ISL_515417, EPI_ISL_515414, EPI_ISL_515415, EPI_ISL_515379, EPI_ISL_515412, EPI_ISL_515413, EPI_ISL_515377, EPI_ISL_515410, EPI_ISL_515378, EPI_ISL_515411, EPI_ISL_515364, EPI_ISL_515365, EPI_ISL_515362, EPI_ISL_515363, EPI_ISL_515360, EPI_ISL_515361, EPI_ISL_515405, EPI_ISL_515406, EPI_ISL_515403, EPI_ISL_515404, EPI_ISL_515368, EPI_ISL_515401, EPI_ISL_515369, EPI_ISL_515402, EPI_ISL_515366, EPI_ISL_515367, EPI_ISL_515400, EPI_ISL_515353, EPI_ISL_515354, EPI_ISL_515351, EPI_ISL_515352, EPI_ISL_515350, EPI_ISL_515359, EPI_ISL_515357, EPI_ISL_515358, EPI_ISL_515355, EPI_ISL_515356, EPI_ISL_515342, EPI_ISL_515343, EPI_ISL_515340, EPI_ISL_515461, EPI_ISL_515341, EPI_ISL_515462, EPI_ISL_515460, EPI_ISL_515348, EPI_ISL_515349, EPI_ISL_515346, EPI_ISL_515347, EPI_ISL_515344, EPI_ISL_515345, EPI_ISL_515331, EPI_ISL_515298, EPI_ISL_515452, EPI_ISL_515332, EPI_ISL_515299, EPI_ISL_515453, EPI_ISL_515296, EPI_ISL_515450, EPI_ISL_515330, EPI_ISL_515297, EPI_ISL_515451, EPI_ISL_515294, EPI_ISL_515295, EPI_ISL_515293, EPI_ISL_515339, EPI_ISL_515337, EPI_ISL_515458, EPI_ISL_515338, EPI_ISL_515459, EPI_ISL_515335, EPI_ISL_515456, EPI_ISL_515336, EPI_ISL_515457, EPI_ISL_515333, EPI_ISL_515454, EPI_ISL_515334, EPI_ISL_515455, EPI_ISL_515319,

EPI_ISL_515320, EPI_ISL_515441, EPI_ISL_515321, EPI_ISL_515442, EPI_ISL_515440, EPI_ISL_515328, EPI_ISL_515449, EPI_ISL_515329, EPI_ISL_515326, EPI_ISL_515447, EPI_ISL_515327, EPI_ISL_515448, EPI_ISL_515324, EPI_ISL_515445, EPI_ISL_515325, EPI_ISL_515446, EPI_ISL_515322, EPI_ISL_515443, EPI_ISL_515323, EPI_ISL_515444, EPI_ISL_515308, EPI_ISL_515429, EPI_ISL_515309, EPI_ISL_515390, EPI_ISL_515397, EPI_ISL_515430, EPI_ISL_515310, EPI_ISL_515398, EPI_ISL_515431, EPI_ISL_515395, EPI_ISL_515396, EPI_ISL_515393, EPI_ISL_515394, EPI_ISL_515391, EPI_ISL_515392, EPI_ISL_515317, EPI_ISL_515438, EPI_ISL_515318, EPI_ISL_515439, EPI_ISL_515315, EPI_ISL_515436, EPI_ISL_515316, EPI_ISL_515437, EPI_ISL_515313, EPI_ISL_515434, EPI_ISL_515314, EPI_ISL_515435, EPI_ISL_515311, EPI_ISL_515399, EPI_ISL_515432, EPI_ISL_515312, EPI_ISL_515433, EPI_ISL_515418, EPI_ISL_515419, EPI_ISL_515386, EPI_ISL_515387, EPI_ISL_515420, EPI_ISL_515384, EPI_ISL_515385, EPI_ISL_515382, EPI_ISL_515383, EPI_ISL_515380, EPI_ISL_515381, EPI_ISL_515306, EPI_ISL_515427, EPI_ISL_515307, EPI_ISL_515428, EPI_ISL_515304, EPI_ISL_515425, EPI_ISL_515305, EPI_ISL_515426, EPI_ISL_515302, EPI_ISL_515423, EPI_ISL_515303, EPI_ISL_515424, EPI_ISL_515300, EPI_ISL_515388, EPI_ISL_515421, EPI_ISL_515301, EPI_ISL_515389, EPI_ISL_515422

ACKNOWLEDGEMENTS:

We thank the staff at the Nevada State Public Health Lab (NSPHL). This work was supported by NSPHL, University of Nevada, Reno Vice President for Research and Innovation (VPRI), Department of Microbiology & Immunology, UNR School of Medicine, Nevada IDeA Network of Biomedical Research Excellence (INBRE) from the National Institute of General Medical Sciences (GM 103440 and GM 104944) from the National Institutes of Health (NIH). The authors wish to acknowledge the support of Research & Innovation and the Office of Information Technology at the University of Nevada, Reno for computing time on the Pronghorn High-Performance Computing Cluster.

AUTHOR CONTRIBUTION:

PDH: conceptualization, formal analysis, methodology, writing – original draft preparation, writing – review and editing

RLT: conceptualization, formal analysis, methodology, writing – original draft preparation, writing – review and editing

XY: formal analysis, writing – review and editing

DPA: conceptualization, funding

JRS: formal analysis, writing – review and editing

AG: methodology

MP: conceptualization, formal analysis, methodology, project administration, funding, writing – review and editing

CCR: conceptualization, formal analysis, methodology, project administration, funding, writing – original draft preparation, writing – review and editing

SCV: conceptualization, formal analysis, methodology, project administration, funding, writing – review and editing

414 **DECLARATIONS:**

415 **Ethics Approval:**

416 Deidentified human specimens (nasal and nasopharyngeal swabs) were used for the
417 extraction of viral RNA all the experiments were done in accordance with guidelines of
418 the University of Nevada, Reno. The University of Nevada, Reno Institutional Review
419 Board (IRB) reviewed this project and determined this study to be EXEMPT FROM IRB
420 REVIEW according to federal regulations and University policy.

421 The Environmental and Biological Safety committee of the University of Nevada, Reno,
422 approved methods and techniques used in this study.

423 **Competing Interests:**

424 The authors declare that they have no competing interests with the contents of this article.

425

426 **REFERENCES:**

427 1. Coronaviridae Study Group of the International Committee on Taxonomy of V: **The**
428 **species Severe acute respiratory syndrome-related coronavirus: classifying**
429 **2019-nCoV and naming it SARS-CoV-2**. *Nat Microbiol* 2020, **5**(4):536-544.

430 2. Petrosillo N, Viceconte G, Ergonul O, Ippolito G, Petersen E: **COVID-19, SARS**
431 **and MERS: are they closely related?** *Clin Microbiol Infect* 2020, **26**(6):729-734.

432 3. Zhou P, Yang XL, Wang XG, Hu B, Zhang L, Zhang W, Si HR, Zhu Y, Li B, Huang
433 CL *et al*: **A pneumonia outbreak associated with a new coronavirus of**
434 **probable bat origin**. *Nature* 2020, **579**(7798):270-273.

435 4. Hu D, Zhu C, Ai L, He T, Wang Y, Ye F, Yang L, Ding C, Zhu X, Lv R *et al*: **Genomic**
436 **characterization and infectivity of a novel SARS-like coronavirus in Chinese**
437 **bats**. *Emerg Microbes Infect* 2018, **7**(1):154.
438 5. de Wit E, van Doremalen N, Falzarano D, Munster VJ: **SARS and MERS: recent**
439 **insights into emerging coronaviruses**. *Nat Rev Microbiol* 2016, **14**(8):523-534.
440 6. Peiris JS, Lai ST, Poon LL, Guan Y, Yam LY, Lim W, Nicholls J, Yee WK, Yan
441 WW, Cheung MT *et al*: **Coronavirus as a possible cause of severe acute**
442 **respiratory syndrome**. *Lancet* 2003, **361**(9366):1319-1325.
443 7. Zaki AM, van Boheemen S, Bestebroer TM, Osterhaus AD, Fouchier RA: **Isolation**
444 **of a novel coronavirus from a man with pneumonia in Saudi Arabia**. *N Engl J*
445 *Med* 2012, **367**(19):1814-1820.
446 8. Zhong NS, Zheng BJ, Li YM, Poon, Xie ZH, Chan KH, Li PH, Tan SY, Chang Q,
447 Xie JP *et al*: **Epidemiology and cause of severe acute respiratory syndrome**
448 **(SARS) in Guangdong, People's Republic of China, in February, 2003**. *Lancet*
449 2003, **362**(9393):1353-1358.
450 9. Kim D, Lee JY, Yang JS, Kim JW, Kim VN, Chang H: **The Architecture of SARS-**
451 **CoV-2 Transcriptome**. *Cell* 2020, **181**(4):914-921 e910.
452 10. Licastro D, Rajasekharan S, Dal Monego S, Segat L, D'Agaro P, Marcello A:
453 **Isolation and Full-Length Genome Characterization of SARS-CoV-2 from**
454 **COVID-19 Cases in Northern Italy**. *J Virol* 2020, **94**(11).
455 11. Holland LA, Kaelin EA, Maqsood R, Estifanos B, Wu LI, Varsani A, Halden RU,
456 Hogue BG, Scotch M, Lim ES: **An 81-Nucleotide Deletion in SARS-CoV-2**

457 **ORF7a Identified from Sentinel Surveillance in Arizona (January to March**
458 **2020)**. *J Virol* 2020, **94**(14).
459 12. Wu F, Zhao S, Yu B, Chen YM, Wang W, Song ZG, Hu Y, Tao ZW, Tian JH, Pei
460 YY *et al*: **A new coronavirus associated with human respiratory disease in**
461 **China**. *Nature* 2020, **579**(7798):265-269.
462 13. Davidson AD, Williamson MK, Lewis S, Shoemark D, Carroll MW, Heesom KJ,
463 Zambon M, Ellis J, Lewis PA, Hiscox JA *et al*: **Characterisation of the**
464 **transcriptome and proteome of SARS-CoV-2 reveals a cell passage induced**
465 **in-frame deletion of the furin-like cleavage site from the spike glycoprotein**.
466 *Genome Med* 2020, **12**(1):68.
467 14. Walls AC, Park YJ, Tortorici MA, Wall A, McGuire AT, Veesler D: **Structure,**
468 **Function, and Antigenicity of the SARS-CoV-2 Spike Glycoprotein**. *Cell* 2020,
469 **181**(2):281-292 e286.
470 15. Bolger AM, Lohse M, Usadel B: **Trimmomatic: a flexible trimmer for Illumina**
471 **sequence data**. *Bioinformatics* 2014, **30**(15):2114-2120.
472 16. Langmead B, Salzberg SL: **Fast gapped-read alignment with Bowtie 2**. *Nat*
473 *Methods* 2012, **9**(4):357-359.
474 17. Picard-Toolkit.: **[cited 17 Aug 2020]**. *In: Github [Internet]* 2019, **Available:**
475 **http://broadinstitute.github.io/picard**.
476 18. Garrison E, Marth G: **Haplotype-based variant detection from short-read**
477 **sequencing**. *arXiv [q-bioGN]* 2012, **Available: http://arxiv.org/abs/1207.3907**.
478 19. Garrison E: **Vcflib: A C++ library for parsing and manipulating VCF files**.
479 *Available: https://githubcom/vcflib/vcflib* 2019.

480 20. Li H: **A statistical framework for SNP calling, mutation discovery, association**
481 **mapping and population genetical parameter estimation from sequencing**
482 **data**. *Bioinformatics* 2011, **27**(21):2987-2993.
483 21. Elbe S, Buckland-Merrett G: **Data, disease and diplomacy: GISAID's innovative**
484 **contribution to global health**. *Glob Chall* 2017, **1**(1):33-46.
485 22. Nextstrain.: **Genomic epidemiology of novel coronavirus - Global**
486 **subsampling**. *In: Nextstrainorg [Internet] 15 Jul 2020 [cited 15 Jul 2020]* 2020,
487 **Available: https://nextstrain.org/ncov/global/2020-07-**
488 **15?d=tree&l=clock&legend=closed**.
489 23. Hadfield J, Megill C, Bell SM, Huddleston J, Potter B, Callender C, Sagulenko P,
490 Bedford T, Neher RA: **Nextstrain: real-time tracking of pathogen evolution**.
491 *Bioinformatics* 2018, **34**(23):4121-4123.
492 24. Chen J, Malone B, Llewellyn E, Grasso M, Shelton PMM, Olinares PDB, Maruthi
493 K, Eng ET, Vatandaslar H, Chait BT *et al*: **Structural Basis for Helicase-**
494 **Polymerase Coupling in the SARS-CoV-2 Replication-Transcription**
495 **Complex**. *Cell* 2020.
496 25. Korber B, Fischer WM, Gnanakaran S, Yoon H, Theiler J, Abfalterer W, Hengartner
497 N, Giorgi EE, Bhattacharya T, Foley B *et al*: **Tracking Changes in SARS-CoV-2**
498 **Spike: Evidence that D614G Increases Infectivity of the COVID-19 Virus**. *Cell*
499 2020, **182**(4):812-827 e819.
500 26. Nextclade: **[cited 17 Aug 2020]**. *Available: https://cladesnextstrainorg* 2020.
501 27. Matranga CB, Andersen KG, Winnicki S, Busby M, Gladden AD, Tewhey R,
502 Stremlau M, Berlin A, Gire SK, England E *et al*: **Enhanced methods for unbiased**

503 **deep sequencing of Lassa and Ebola RNA viruses from clinical and**
504 **biological samples**. *Genome Biol* 2014, **15**(11):519.
505 28. Briese T, Kapoor A, Mishra N, Jain K, Kumar A, Jabado OJ, Lipkin WI: **Virome**
506 **Capture Sequencing Enables Sensitive Viral Diagnosis and Comprehensive**
507 **Virome Analysis**. *mBio* 2015, **6**(5):e01491-01415.
508 29. O'Flaherty BM, Li Y, Tao Y, Paden CR, Queen K, Zhang J, Dinwiddie DL, Gross
509 SM, Schroth GP, Tong S: **Comprehensive viral enrichment enables sensitive**
510 **respiratory virus genomic identification and analysis by next generation**
511 **sequencing**. *Genome Res* 2018, **28**(6):869-877.
512 30. Paden CR, Tao Y, Queen K, Zhang J, Li Y, Uehara A, Tong S: **Rapid, Sensitive,**
513 **Full-Genome Sequencing of Severe Acute Respiratory Syndrome**
514 **Coronavirus 2**. *Emerg Infect Dis* 2020, **26**(10).
515 31. Paskey AC, Frey KG, Schroth G, Gross S, Hamilton T, Bishop-Lilly KA:
516 **Enrichment post-library preparation enhances the sensitivity of high-**
517 **throughput sequencing-based detection and characterization of viruses**
518 **from complex samples**. *BMC Genomics* 2019, **20**(1):155.
519 32. Xiao M, Liu X, Ji J, Li M, Li J, Yang L, Sun W, Ren P, Yang G, Zhao J *et al*: **Multiple**
520 **approaches for massively parallel sequencing of SARS-CoV-2 genomes**
521 **directly from clinical samples**. *Genome Med* 2020, **12**(1):57.
522
523
524
525

526 **FIGURE LEGENDS:**

527 **Figure 1. Workflow of SARS-CoV-2 genome sequencing and analysis from**
528 **nasopharyngeal patient specimens in Nevada.** (A) RNA was extracted from Nasal or
529 Nasopharygeal (NP) swabs taken from patients in Nevada and first used to determine the
530 presence of SARS-CoV-2 genomes by RT-qPCR. Next generation sequencing (NGS)
531 libraries were prepared from positive specimens, this included steps for ribosomal RNA
532 depletion and SARS-CoV-2 enrichment. Subsequent libraries were pooled and used for
533 whole genome sequencing at the Nevada Genomics Center on the Illumina NextSeq 500
534 instrument. FASTQ files were aligned to the reference genome, and analyzed to
535 determine nucleotide variation and phylogenetic relationship. (B) A total of 200 specimens
536 were sequenced, of which 174 had over 99% coverage of the SARS-CoV-2 genome.
537 This included 133 patient specimens from Northern Nevada, 40 from Southern Nevada
538 and 1 specimen that was re-sequenced. (C) Correlation between RT-qPCR Ct value and
539 the percentage of coverage in the whole genome sequencing after trimming and
540 alignment. (D) Nucleotide variants across the SARS-CoV-2 genome in the 173 specimens
541 from Nevada from March 6th to June 5th.

542

543 **Figure 2. Distribution of D614G in Nevada and comparison with the United States**
544 **and global proportion.** (A) Cumulative frequency of D614G in 173 patient specimens
545 from Nevada from March 6th to June 5th, 2020 (D614 is indicated by teal, G614 is
546 indicated by yellow). Pie charts depict the cumulative proportion up to the indicated time
547 point (March 15, April 1, May 1, June 5). The total number of specimens included at each
548 time point is specified below each pie chart. Effective dates of emergency orders and

549 regulatory responses to SARS-CoV-2 spread in Nevada are indicated on the frequency
550 graph time axis. (B) Proportion of D614G in the United States from March 6th to June 5th,
551 specimens from Nevada are divided in the geographic area that they originated from,
552 Northern Nevada (N-NV) includes 133 specimens from Washoe county, Carson-Tahoe,
553 and other northern counties, and Southern Nevada (S-NV) includes 40 specimens from
554 Clark county. (C) Global proportion of D614G in the shown regions during the same time
555 period from a subsampling of sequences deposited in Nextstrain.org. The size of the pie
556 chart corresponds to the relative specimen number for each region.
557
558 **Figure 3. Distribution of SARS-CoV-2 clades in Nevada.** (A) Cumulative frequency of
559 SARS-CoV-2 clades in 173 patient specimens from Nevada during March 6th to June
560 5th. The five clades are colored 19A (blue), 19B (teal), 20A (green), 20B (yellow) and 20C
561 (orange). Pie charts depict the cumulative proportion up to the indicated time point (March
562 15, April 1, May 1, June 5). The total number of specimens included at each time point is
563 specified below each pie chart. Dates of emergency orders and regulations meant to slow
564 the spread of SARS-CoV-2 in Nevada are indicated on the time scale of the frequency
565 graph. (B) Circular dendrogram depicting clades from Nevada specimens. (C) Pie chart
566 of the clades from northern Nevada (N-NV), southern Nevada (S-NV) and the United
567 States. (D) Pie charts show the proportion of clades from global regions during the same
568 time period from a subsampling of sequences deposited in Nextstrain.org. The size of the
569 pie chart corresponds to the relative specimen number for each region.
570

571 **Figure 4. Distribution of P323L/F (nsp12, RdRp) in Nevada.** (A) Cumulative frequency
572 of P323L/F (nsp12, RdRp) in 173 patient specimens from Nevada during March 6th to
573 June 5th. The amino acid at position 323 is indicated by teal for proline (P), yellow for
574 leucine (L) and blue for phenylalanine (F). Pie charts depict the cumulative proportion up
575 to the indicated time point (March 15, April 1, May 1, June 5). The total number of
576 specimens included at each time point is specified below each pie chart. Dates of
577 emergency orders and regulations meant to slow the spread of SARS-CoV-2 in Nevada
578 are indicated on the time scale of the frequency graph. (B) Circular dendrogram
579 representing the distribution of amino acid change at residue 323 of nsp12 from a global
580 subsampling of sequences deposited in Nextstrain.org from March 6th to June 5th, the
581 larger dots indicate specimens from Nevada. (C) Pie chart indicating the ratio of P/L/F in
582 Northern NV and Southern NV specimens from this study. (D) Proportion of P323L/F from
583 a subsampling of sequences deposited in Nextstrain.org for the United States and (E)
584 global regions from March 6th to June 5th. The size of the pie chart corresponds to the
585 relative specimen number for each region.
586
587
588 **SUPPLEMENTARY FIGURES**
589 **Figure S1. Alignment of SARS-CoV-2 sequences from NV patient's specimens.**
590 SARS-CoV-2 sequences from patient specimen were aligned together with the original
591 COVID-19 sequence from Wuhan, NC_045512.2, using multiple sequences alignment
592 tool MUSCLE 3.8.31. The aligned sequences were sorted based on number of Ns in
593 each sequence from the smallest to the largest. The sorted alignment file in aln format

594 was uploaded to the web portal of NCBI Multiple Sequence Alignment Viewer, Version
595 1.15.0, for visualization.
596
597 **Figure S2. Dendrogram of Nevada specimens in context of other sequenced**
598 **specimens.** (a) Nucleotide mutation clock from Nextstrain.org with the SARS-CoV-2
599 genome isolated from Washington (USA/WA 1/2020) on January 24th and first specimen
600 from Nevada (A0004) on March 5th indicated in red. (b) Circular dendrogram of Nevada
601 specimens from March 6th to June 5th positioned within a subsample of global sequences
602 from Nextstrain.org during the same time period, the larger dots indicate specimens from
603 Nevada. The five clades are colored 19A (blue), 19B (teal), 20A (green), 20B (yellow) and
604 20C (orange).
605
606 **Figure S3. Global distribution of clades from March 6th to June 5th.** Pie charts depict
607 the proportion of the clades within (a) four main areas in Nevada, these include 91
608 specimens from Washoe county (upper left), 23 specimens from Carson-Tahoe (middle
609 left), 40 specimens from Clark county (bottom right), and 19 from rural Nevada (middle).
610 The five clades are colored 19A (blue), 19B (teal), 20A (green), 20B (yellow) and 20C
611 (orange). (b) Pie chart of the clades in each indicated country from March 6th to June 5th
612 generated from a subsampling of sequences deposited in Nextstrain.org. The size of the
613 pie chart corresponds to the relative specimen number for each region.
614
615 **Figure S4. Distribution of nucleotide variant 379C>A.** (a) Green line at the far-left end
616 of the genome denoted nucleotide position 379 of nsp1. (b) Circular dendrogram of global

617 subsample of sequences from Nextstrain.org with NV specimens indicated by larger dots.
618 (c) Pie chart indicating the proportion of sequences with either the cytidine (C) or
619 adenosine (A) at position 379 from the Nevada specimens. Subsample of sequences from
620 Nextstrain.org were used to generate the proportion of 379C>A in (d) the indicated states
621 within the U.S. and (e) internationally. The size of the pie chart corresponds to the relative
622 specimen number for each region.
623
624 **Figure S5. Structure of SARS-CoV-2 nsp12 (RdRp) P323L/F.** (a) Diagram depicting
625 ORF1b genomic location and encoded proteins. Below the linear protein schematic of
626 nsp12 specific nucleotide variants at position 14,407 and 14,408 and the resulting amino
627 acid changes are indicated. (b) SARS-CoV-2 replicase complex modeled from 6XEZ
628 template. This model includes nsp12, nsp7, nsp8, nsp13, ligands (ZN, Mg), the template
629 and product strand of RNA. P323L/F within the interface domain of nsp12 is located at
630 the left side of the complex. (c) Model nsp12 showing P323L/F within the interface
631 domain. Residue 323 is shown with either P, L or F and amino acids with side chains
632 within 5 Å of residue 323 are depicted as sticks in the cartoon model.
633

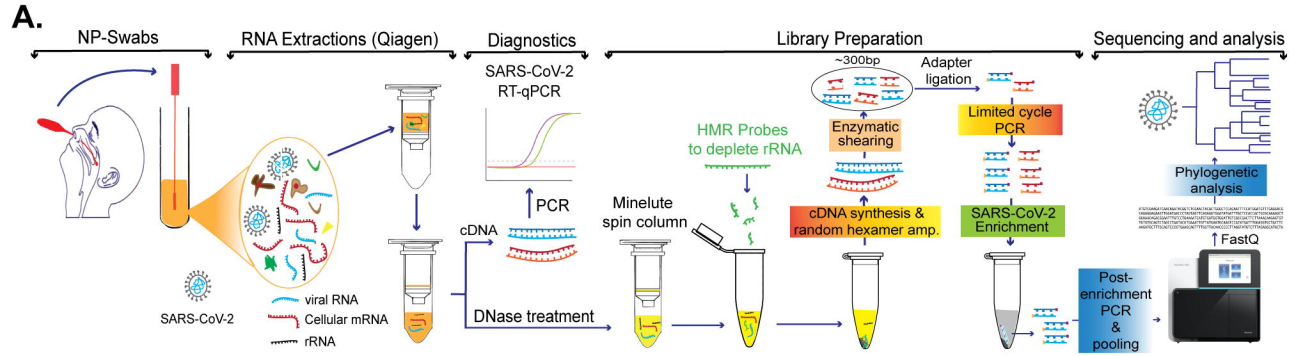

B.

200 Total samples
26 <90% coverage
174 >90% coverage
133 patient samples from Northern Nevada (N-NV)
(Washoe County, Carson-Tahoe area and Other)
40 patient samples from Southern Nevada (S-NV)
(Clark county)
1 Repeat sequencing of specimen

C.

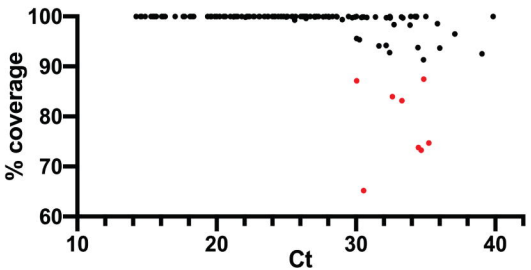

D.

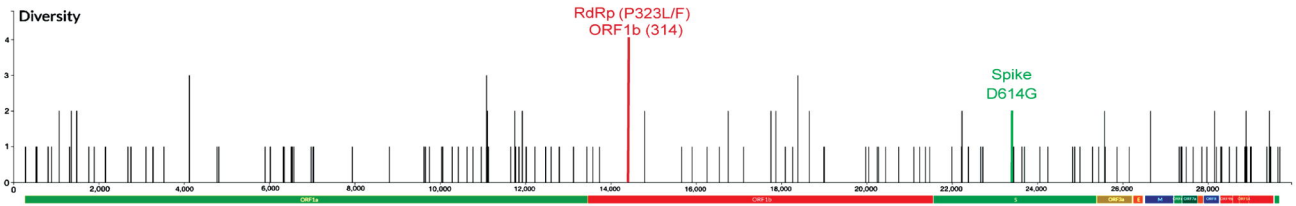

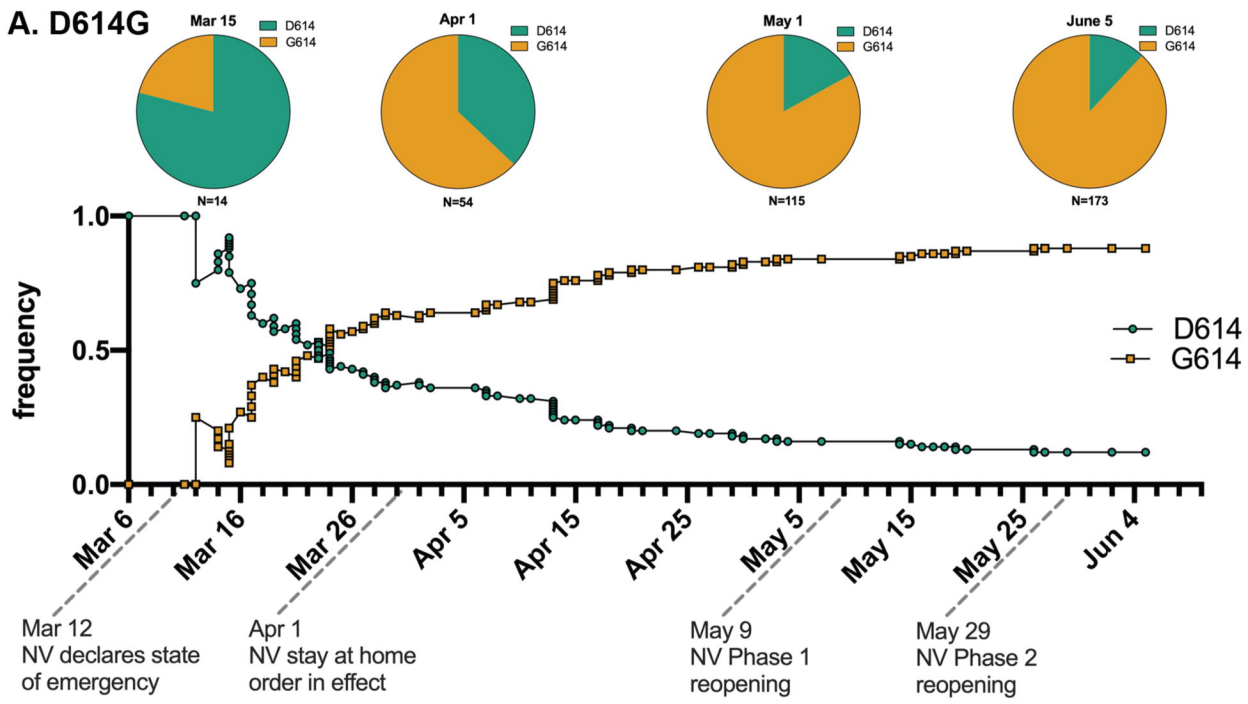
A. D614G
Mar 15
Apr 1
May 1
June 5
D614
G614
N=14
N=54
N=115
N=173
frequency
1.0
0.5
0.0
Mar 6
Mar 16
Mar 26
Apr 5
Apr 15
Apr 25
May 5
May 15
May 25
Jun 4
Mar 12
NV declares state of emergency
Apr 1
NV stay at home order in effect
May 9
NV Phase 1 reopening
May 29
NV Phase 2 reopening

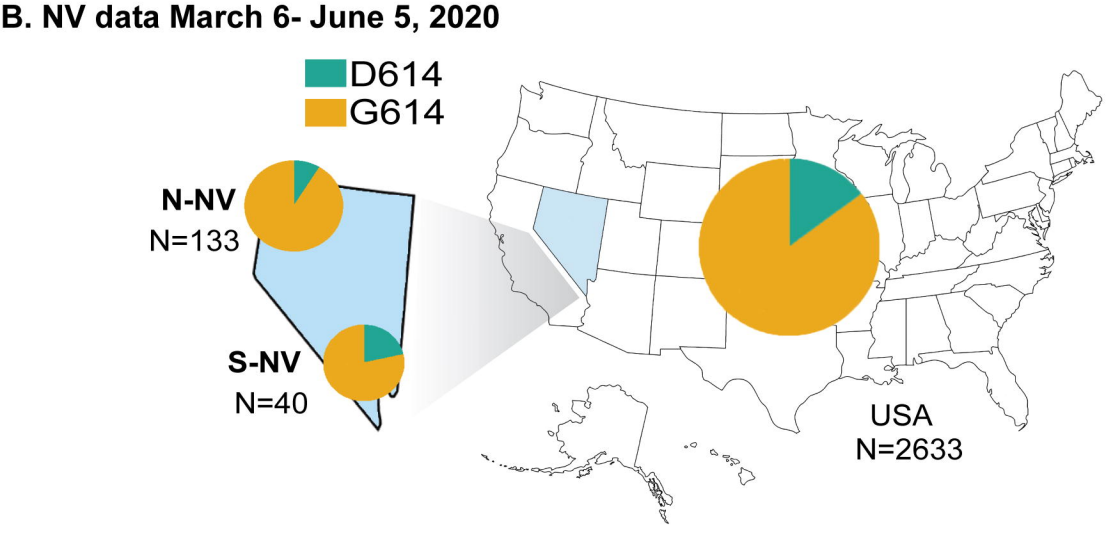
B. NV data March 6- June 5, 2020
D614
G614
N-NV
N=133
S-NV
N=40
USA
N=2633

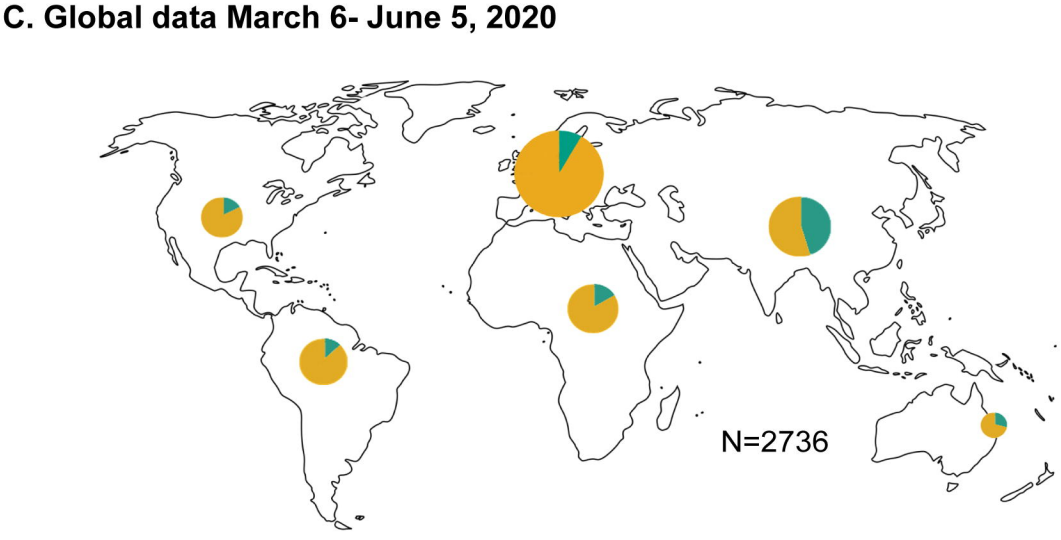
C. Global data March 6- June 5, 2020
N=2736

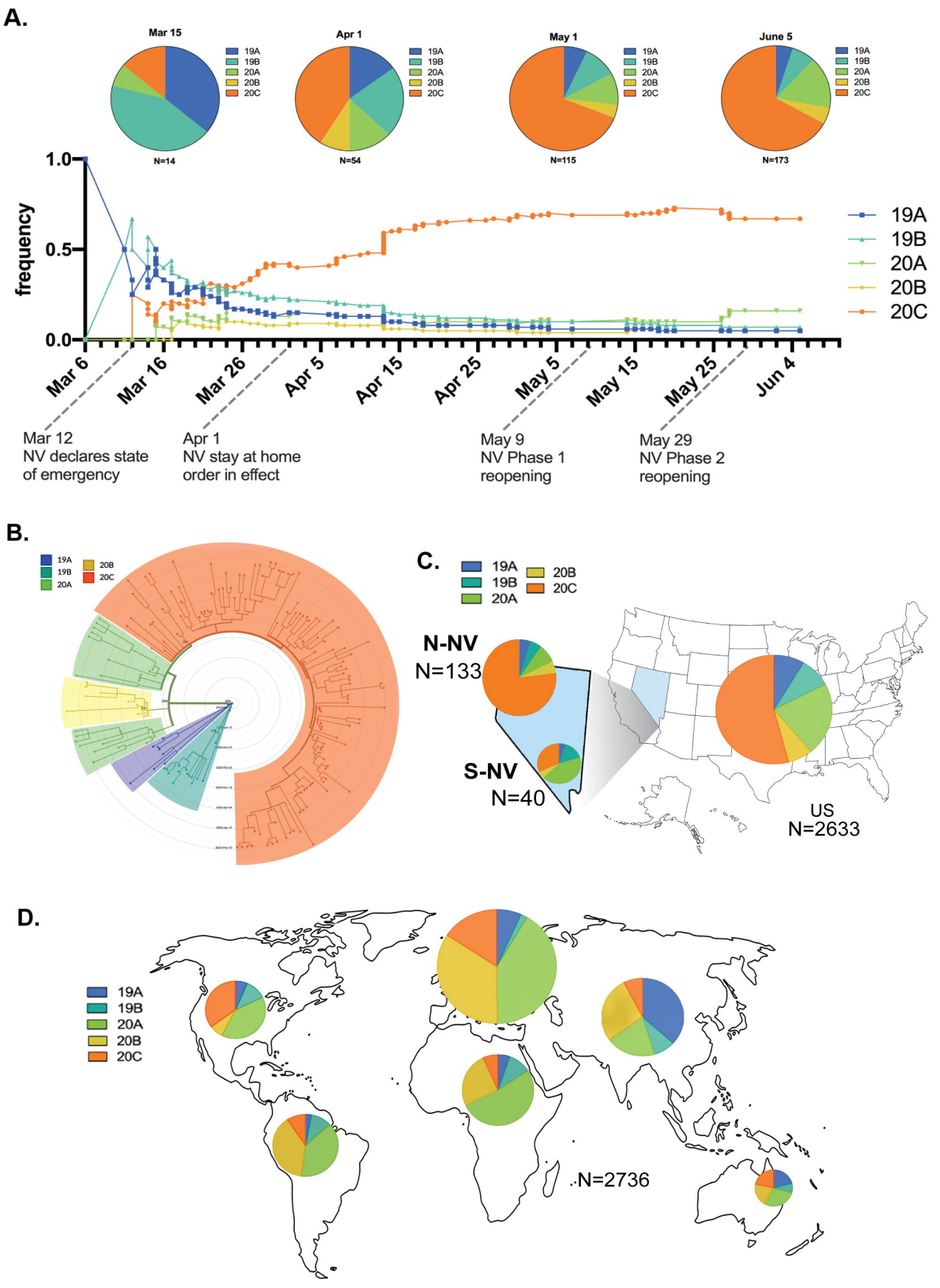
A.
Mar 15
Apr 1
May 1
June 5
19A
19B
20A
20B
20C
N=14
N=54
N=115
N=173
frequency
1.0
0.5
0.0
Mar 6
Mar 16
Mar 26
Apr 5
Apr 15
Apr 25
May 5
May 15
May 25
Jun 4
Mar 12
NV declares state of emergency
Apr 1
NV stay at home order in effect
May 9
NV Phase 1 reopening
May 29
NV Phase 2 reopening
B.
C.
N-NV
N=133
S-NV
N=40
US
N=2633
D.
N=2736

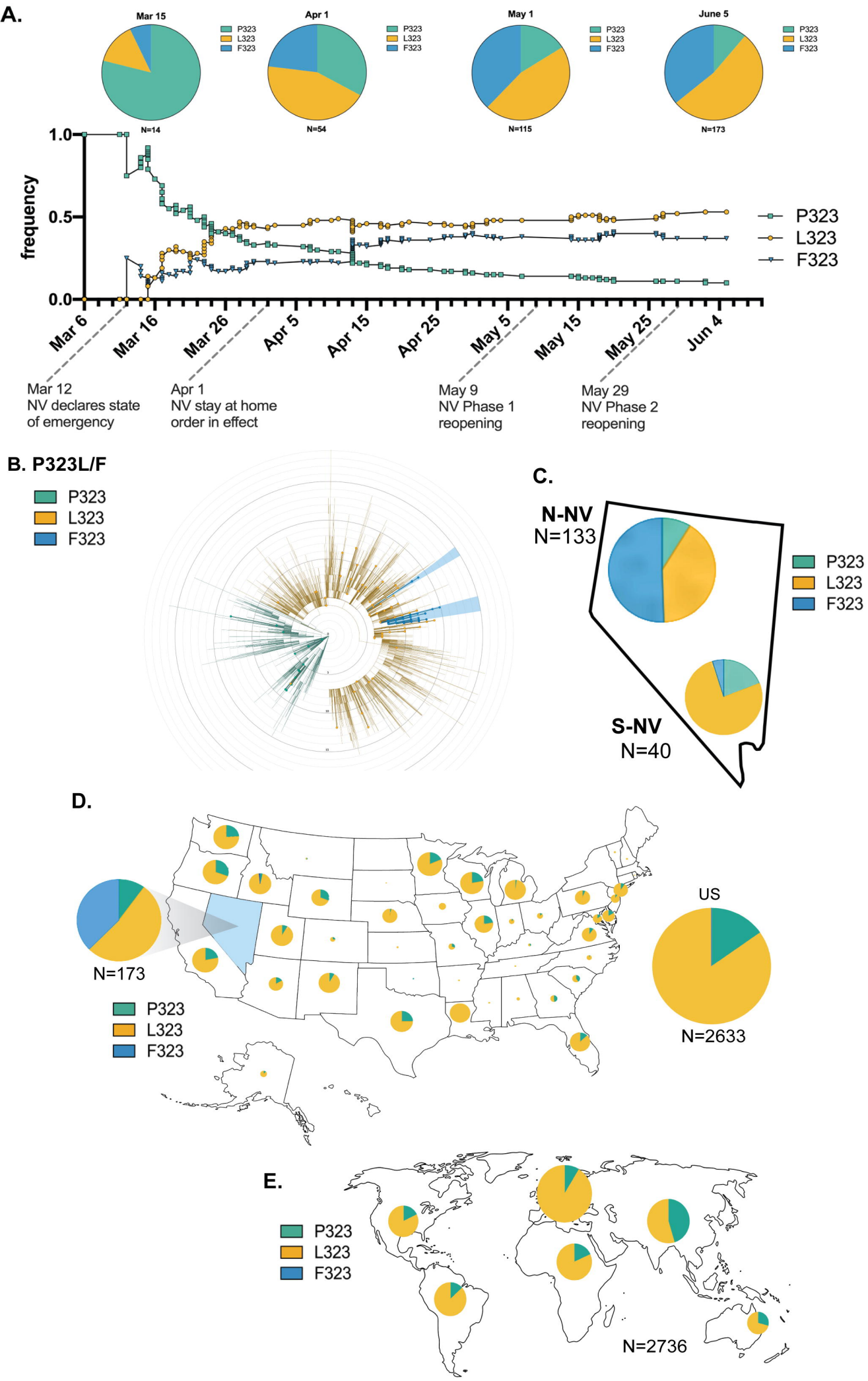
A.
Mar 15
Apr 1
May 1
June 5
P323
L323
F323
N=14
N=54
N=115
N=173
frequency
1.0
0.5
0.0
Mar 6
Mar 16
Mar 26
Apr 5
Apr 15
Apr 25
May 5
May 15
May 25
Jun 4
Mar 12
NV declares state of emergency
Apr 1
NV stay at home order in effect
May 9
NV Phase 1 reopening
May 29
NV Phase 2 reopening
B. P323L/F
P323
L323
F323
C.
N-NV
N=133
S-NV
N=40
P323
L323
F323
D.
N=173
P323
L323
F323
US
N=2633
E.
P323
L323
F323
N=2736